A Model for 8–10 Hz Spindling in Interconnected Thalamic Relay and Reticularis Neurons

A. Destexhe,* D. A. McCormick,‡ and T. J. Sejnowski*

*Howard Hughes Medical Institute and The Salk Institute, Computational Neurobiology Laboratory, La Jolla, California 92037, and ‡Section of Neurobiology, Yale University School of Medicine, New Haven Connecticut 06510 USA

ABSTRACT We investigated a simplified model of a thalamocortical cell and a reticular thalamic cell interconnected with excitatory and inhibitory synapses, based on Hodgkin-Huxley type kinetics. The intrinsic oscillatory properties of the model cells were similar to those observed from single cells in vitro. When synaptic interactions were included, spindle oscillations were observed consisting of sequences of rhythmic oscillations at 8–10 Hz separated by silent periods of 8–40 s. The model suggests that Ca^{2+} regulation of I_h channels may be responsible for the waxing and waning of spindles and that the reticular cell shapes the 10-Hz rhythmicity. The model also predicts that the kinetics of γ-aminobutyric acid inhibitory postsynaptic potentials as well as the intrinsic properties of reticular cells are critical in determining the frequency of spindle rhythmicity.

INTRODUCTION

Spindle oscillations are waxing and waning 7–14-Hz waves that originate in the thalamus during slow-wave sleep in mammals (reviewed in Steriade and Deschênes, 1984; Steriade and Llinàs, 1988). Recently, spindle oscillations have also been demonstrated in vitro from thalamic slices that include thalamocortical (TC) and reticular (RE) thalamic cells (von Krosigk et al., 1993). These in vitro spindles consisted of sequences of 5–9-Hz rhythmic bursting separated by silent periods of 3–30 s. The occurrence of these spindles depended critically on the presence of the synaptic connections between TC and RE cells.

Single thalamic neurons have intrinsic properties which include spontaneous oscillatory behavior. Cat and rat TC neurons display spontaneous slow oscillations in the δ frequency range (0.5–4 Hz) (Leresche et al., 1991; McCormick and Pape, 1990; Curró Dossi et al., 1992). In cat relay cells, waxing and waning slow oscillations (0.5–3.2 Hz) can appear as bursts separated by silent periods of about 5–25 s and have been called "spindle-like oscillations" (Leresche et al., 1991), although they differ from spindles in many respects. Rodent RE cells also display rhythmic oscillations at 7–12 Hz after injection of current pulses (Avanzini et al., 1989; Bal and McCormick, 1993). These various types of oscillations are resistant to tetrodotoxin due to mechanisms intrinsic to the cell.

The intrinsic properties of TC and RE cells are difficult to reconcile with the 6–9-Hz spindle oscillations observed in the same neurons when their interconnections were preserved. The neurons are part of a neuronal network: the TC cells make excitatory synapses on RE cells, which in turn make inhibitory synapses back onto TC cells as well as on other RE cells. In this paper, we investigate the effects of synaptic interactions on these intrinsic oscillatory properties and analyze the conditions that produce oscillations in the frequency range of spindling.

MATERIALS AND METHODS

The TC cell and the RE thalamic cell were modeled by single compartments of 1000 μm^2 and Hodgkin-Huxley type of kinetics for the intrinsic currents.

The equations used for describing the time evolution of the membrane potential were

$$C_m \dot{V}_T = -g_L(V_T - E_T) - I_T - I_h - I_{Na} - I_K - I_{GABA} \quad (1)$$

$$C_m \dot{V}_R = -g_L(V_T - E_R) - I_{Ts} - I_{K[Ca]} - I_{CAN} - I_{Na} - I_K - I_{GLU} \quad (2)$$

where V_T and V_R are the membrane potentials of the TC and RE cells, respectively; $C_m = 1\ \mu F/cm^2$ is the specific capacity of the membrane; $g_L = 0.05$ mS/cm^2 is the leakage conductance; $E_T = -86$ mV and $E_R = -80$ mV are the leakage reversal potentials.

Thalamic neurons are characterized by numerous voltage-dependent currents (Jahnsen and Llinàs, 1984), but our goal was to find the minimal number of ionic mechanisms that account for spindling. These currents were the low-threshold Ca^{2+} currents I_T and I_{Ts}, the hyperpolarization-activated current I_h, the Ca^{2+}-activated currents $I_{K[Ca]}$ and I_{CAN}, the fast Na^+ and K^+ currents I_{Na} and I_K responsible for the generation of action potentials, and the synaptic currents I_{GABA} and I_{GLU}.

Each of these currents was modeled by

$$I_i = \bar{g}_i m^M h^N (V - E_i) \quad (3)$$

where $\bar{g}_i$ is the maximal conductance of the current I_i; m and h are the activation and inactivation variables, respectively; M and N are their respective (integer) exponents; V represents either V_T or V_R; and E_i is the reversal potential.

Synaptic currents were modeled by a kinetic scheme for the binding of neurotransmitter to postsynaptic receptors (Destexhe et al., 1994) ($M = 1$ and $N = 0$ in Eq. 3). The fraction of postsynaptic receptors in the open state, m, obeys

$$\frac{dm}{dt} = \alpha[T](1 - m) - \beta m \quad (4)$$

where $[T]$ is the concentration of neurotransmitter in the synapse and α and

Received for publication 16 July 1993 and in final form 2 September 1993

Address reprint requests to Dr. Alain Destexhe, The Salk Insitute, Computational Neurobiology Laboratory, 10010 North Torrey Pines Road, La Jolla, CA 92037. Tel.: 619-453-4100 (ext. 527); Fax: 619-587-0417; email: alain@helmholtz.sdsc.edu.

Abbreviations used: TC, thalamocortical; RE, reticularis; GABA, γ-aminobutyric acid; PSP, postsynaptic potential; IPSP, inhibitory postsynaptic potential.

0006-3495/93/12/2473/05 $2.00

β are forward and backward binding rates. The neurotransmitter was released in a pulse (1 ms duration, 1 mM amplitude) when a presynaptic spike occurred. This method for computing synaptic currents is more realistic than the traditional α function, and it naturally handles summation of PSPs (Destexhe et al., 1994).

For the TC cell, the kinetic equations used for describing the activation and inactivation variables of the currents have already been described (Destexhe et al., 1993a) and the same model was used here. The I_T kinetics were taken from Wang et al. (1991), and I_h was based on the model of Destexhe and Babloyantz (1993) to which a regulation by intracellular Ca^{2+} was added (Destexhe et al., 1993a).

For the RE cell, I_{Ts} was taken from the voltage clamp data of Huguenard and Prince (1992) using $M = 2$ and $N = 1$. Two Ca^{2+}-dependent currents, the slow K^+ current, $I_{K[Ca]}$, and the slow nonspecific cation current, I_{CAN} affected the oscillatory properties of RE cells (Bal and McCormick, 1993). They are modeled here as voltage-independent currents described by Eq. 3 with $M = 2$ and $N = 0$, similar to Yamada et al. (1989) in bullfrog sympathetic ganglion cells. The activation variable m obeys

$$\dot{m} = \alpha[Ca]_i^2(1 - m) - \beta m \quad (5)$$

where α and β are rate constants and $[Ca]_i$ is the intracellular calcium concentration. Adjustment of the kinetics of these currents to the current clamp data of RE neurons (Bal and McCormick, 1993) gives $\alpha = 48$ ms^{-1} mM^{-2}, $\beta = 0.03$ ms^{-1} for $I_{K[Ca]}$, and $\alpha = 20$ ms^{-1} mM^{-2}, $\beta = 0.002$ ms^{-1} for I_{CAN}.

For both cells, action potentials were modeled by I_{Na} and I_K, as described in Traub and Miles (1991); and intracellular Ca^{2+} clearance was due to a Ca^{2+} pump, as described in Destexhe et al. (1993a).

All simulations were performed using NEURON (Hines, 1993) with the following values for the maximal conductances and reversal potentials: $\bar{g}_{Ca} = 1.75$ mS/cm^2 for I_T and for I_{Ts}, and in both cases, E_{Ca} was obtained from the Nernst relation assuming an external Ca^{2+} concentration of 2 mM; $\bar{g}_h = 0.12$ mS/cm^2 and $E_h = -43$ mV for I_h; $\bar{g}_{K[Ca]} = 10$ mS/cm^2 and $E_K = -95$ mV for $I_{K[Ca]}$; $\bar{g}_{CAN} = 0.25$ mS/cm^2 and $E_{CAN} = -20$ mV for I_{CAN}; $\bar{g}_{Na} = 100$ mS/cm^2 in RE and 30 mS/cm^2 in TC with $E_{Na} = 50$ mV; $\bar{g}_K = 10$ mS/cm^2 in RE and 2 mS/cm^2 in TC for I_K; $\bar{g}_{GLU} = 1$ nS and $E_{GLU} = 0$ mV for I_{GLU}; $\bar{g}_{GABA} = 4$ nS and $E_{GABA} = -80$ mV for I_{GABA}. The rate constants used for computing synaptic currents were $\alpha = 2$ ms^{-1} mM^{-1}, $\beta = 1$ ms^{-1} for glutamate receptors and $\alpha = 2$ ms^{-1} mM^{-1}, $\beta = 0.1$ ms^{-1} for GABA receptors in Eq. 4.

RESULTS

We first describe the properties of single neurons. In isolated TC cells in vitro, I_T and I_h currents produce slow oscillations (McCormick and Pape, 1990; Soltesz et al., 1991) or waxing and waning slow oscillations (Soltesz et al., 1991). In our model, both types of oscillations were present depending on the level of the membrane potential and the maximal conductance of I_h (Destexhe et al., 1993a) (Fig. 1 *A–C*). The waxing and waning of the slow oscillations occurs as intracellular Ca^{2+} binds progressively to I_h channels leading to the cessation of oscillatory behavior and the emergence of a silent period during which the system recovers before oscillations start again (Destexhe et al., 1993a).

In the isolated RE cell, the currents I_{Ts}, $I_{K[Ca]}$ and I_{CAN} reproduced the basic 10-Hz rhythmic burst firing found in these cells in vitro (Avanzini et al., 1989; Bal and McCormick, 1993). Fig. 1 *D* shows a sequence of 8–12-Hz rhythmic bursts in a RE cell in response to a strong hyperpolarizing current pulse. These oscillations are driven by the interaction between I_{Ts} and $I_{K[Ca]}$. During the oscillations, I_{CAN} activated progressively and elicited a short period of tonic activity at the end of the oscillatory sequence.

The connections between the TC and the RE cell are indicated in Fig. 2 *A*. The two synapses were modeled by the kinetic scheme described in Materials and Methods. I_{GABA} and I_{GLU} represent the $GABA_A$ synaptic current (inhibitory synapse from RE to TC) and the glutamate non-*N*-methyl-D-aspartate current (excitatory synapse from RE to TC), respectively, as identified in ferret thalamic slices (von Krosigk et al., 1993). The PSPs corresponding to these currents are shown in Fig. 2 *B*.

With the TC and RE cells interconnected (Fig. 2 *A*), sequences of 8–10-Hz spindle oscillations were observed (Fig. 2 *C*). These 8–10-Hz spindles occurred when the TC cell displayed intrinsic waxing and waning oscillations. The spindle sequence consisted of bursts of 8–10-Hz oscillations lasting a few seconds and separated by silent periods of 8–40 s. The spindle oscillations began in the TC cell in a manner very similar to the waxing and waning slow oscillations of isolated TC cells (compare with Fig. 1 *B*). As the oscillation began, the first burst of spikes in the TC cell elicited a series of excitatory PSPs which activated I_{Ts} in the RE cell. The RE cell started 8–10-Hz bursting and entrained the TC cell to this oscillation, but the feedback of the TC cell was necessary to maintain the 8–10-Hz rhythmicity. At each cycle of the oscillation, Ca^{2+} bound to the I_h channels in the TC cell and shifted the voltage activation curve for I_h, leading to the cessation of oscillations in a manner similar to the waxing and waning slow oscillations in isolated TC cells (see Destexhe et al., 1993a).

The spindle oscillation rode on a depolarizing envelope in the RE cells and a hyperpolarizing envelope in the TC cell (Fig. 2 *C*). Such a mirror image between the two types of cells is characteristic of intracellular recordings made in anesthetized cats in vivo (Steriade and Llinàs, 1988) and in ferret slices in vitro (von Krosigk et al., 1993).

The generation of spindle oscillations depended on the magnitudes of the synaptic conductances. If the glutamatergic or GABAergic conductances were too low, the coupling was insufficient to produce a spindle; if the GABAergic conductance was to high, the system produced a sustained 10-Hz oscillation because the strong hyperpolarization of the TC cells prevented the Ca^{2+}-bound I_h channels to terminate the oscillation; if the glutamatergic conductance was too high, the rapid depolarization of the RE cell led to a rapid burst and a higher frequency of oscillation.

Previous in vitro results demonstrated that blockade of $GABA_A$ synapses by application of bicuculline transformed the spindle behavior by slowing down the frequency to 2–4 Hz (von Krosigk et al., 1993). Application of a $GABA_B$ receptor antagonist abolished these slowed oscillations, indicating that they were mediated by $GABA_B$ IPSPs. We could reproduce a similar type of behavior in the model by slowing down the decay of the GABA synaptic current. The results summarized in Table 1 show that the decay of inhibition (β in Eq. 4) affects the frequency of the spindle oscillations. The

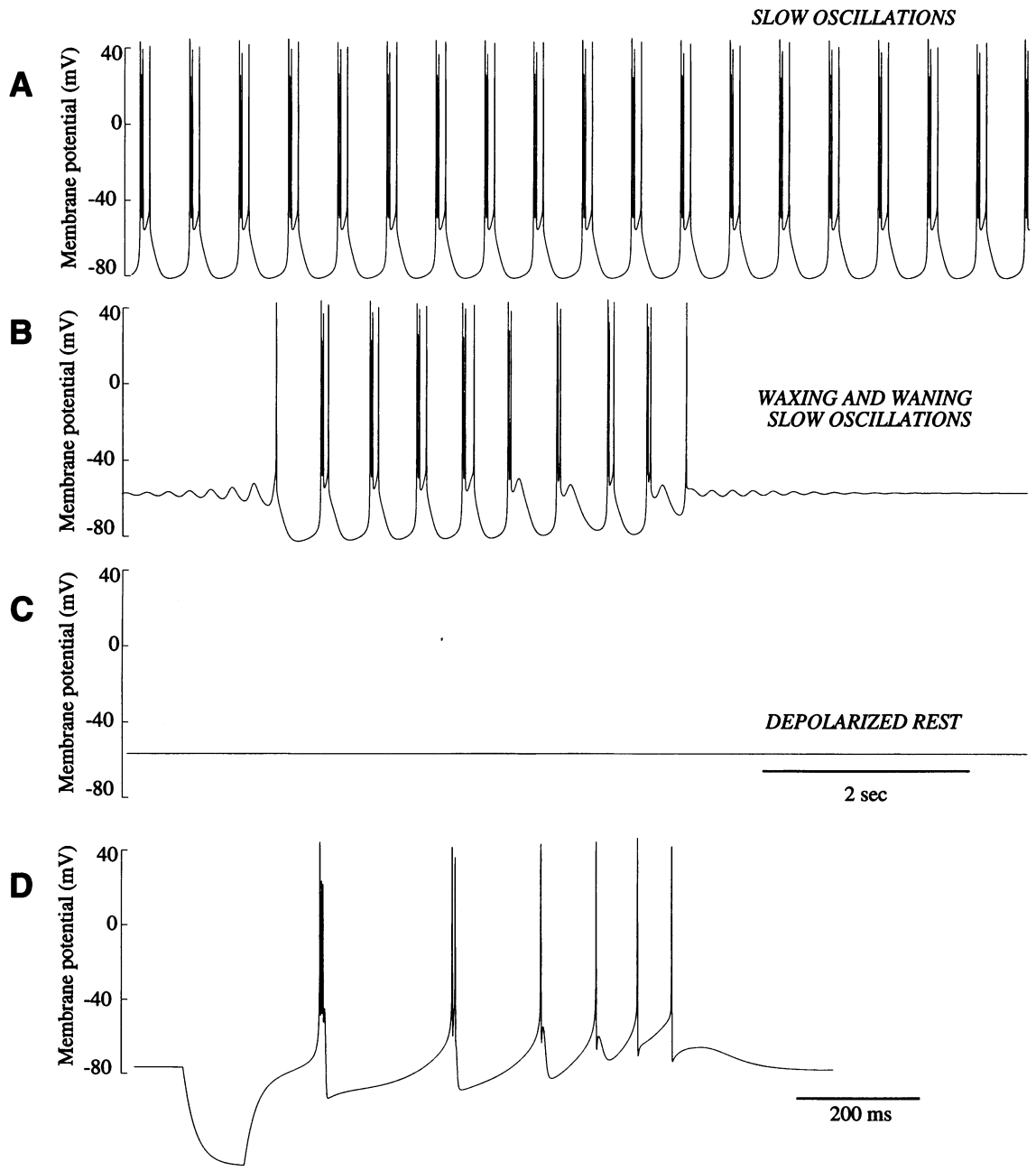

FIGURE 1 Intrinsic oscillating behavior of single TC and RE cells. The model TC cell displays either (*A*) slow oscillations at 0.5–4 Hz, (*B*) waxing and waning slow oscillations at 3.5–4.5 Hz with silent periods of 4–20 s, or (*C*) resting behavior around −60 mV, following the maximal value of the conductance of I_h. ($\bar{g}_h$ = 0.02, 0.05, and 0.2 mS/cm^2, respectively). (*D*) The model RE cell displays bursts of 8–10-Hz oscillations in response to a hyperpolarizing current pulse. Current injected was 0.025 nA during 100 ms.

slower the decay, the lower the frequency, reaching a value close to 3 Hz when the decay was within range the decay time of $GABA_B$ currents (estimated from Otis et al., 1993).

The frequency of spindling depends not only on the decay of IPSPs, but also on the intrinsic properties of the RE cell. In the model of a single RE cell, blocking I_{CAN} resulted in a marked slowing down of the frequency of oscillation (not shown here). When I_{CAN} was blocked in the coupled system during spindle oscillations, the frequency also decreased markedly (Table 1). In addition, there was an increase of the burst after hyperpolarization in the RE cell (not shown).

DISCUSSION

Our simplified model of two thalamic neurons is limited in several respects, because only the primary intrinsic currents were included to account for the main features of the oscillatory properties of these cells, as determined by in vitro

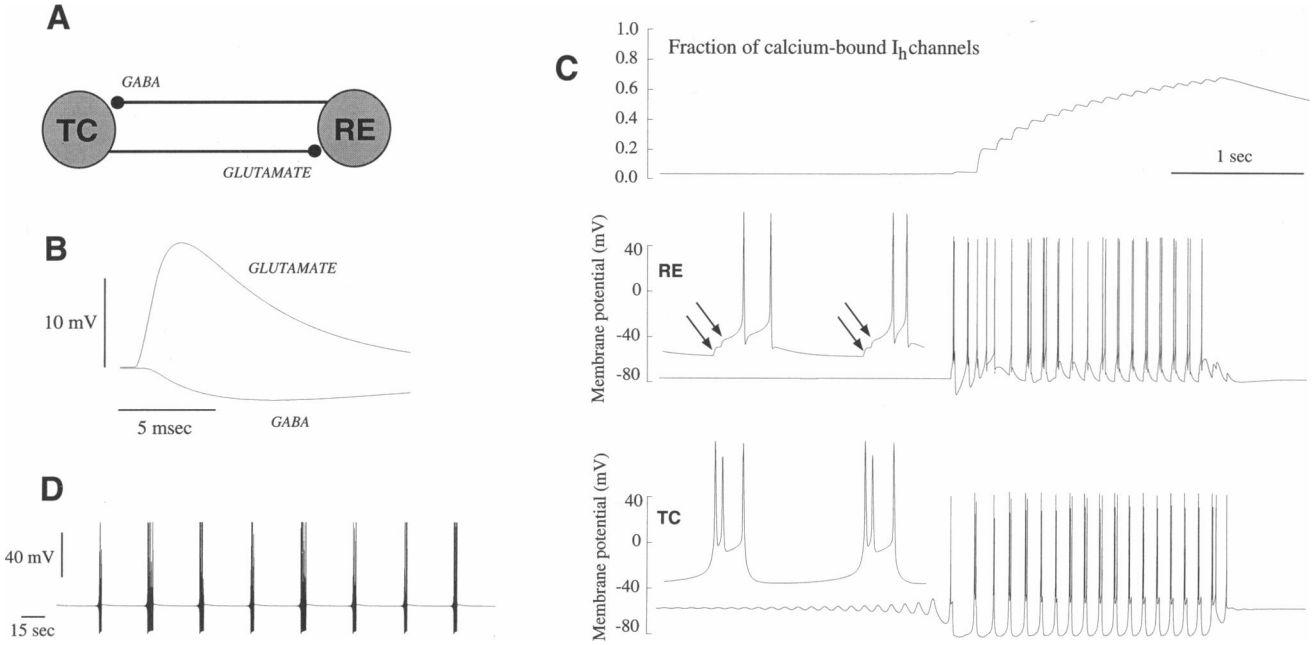

FIGURE 2 Model of 8–10-Hz spindling in interconnected TC and RE cells. (*A*) Schematic drawing of the connections between the two cells. (*B*) Excitatory (glutamate) and inhibitory (GABA) postsynaptic potentials. (*C*) Sequence of spindle oscillations obtained after connection of a TC and a RE cell. The fraction of I_h channels bound to intracellular Ca^{2+}, the membrane potential of RE and TC cells are shown from top to bottom. For each cell, an inset shows two bursts at higher temporal resolution (× 10). Excitatory postsynaptic potentials on the RE cell are indicated by arrows. (*D*) Sequences of spindling in a model TC cell on a longer time scale.

TABLE 1 Frequency of spindling for different values of the decay of inhibitory synaptic currents and I_{CAN} conductance

β (ms^{-1})	Frequency (Hz)
0.1	10.0
0.03	9.0
0.01	5.5
0.005	3.6
0.003	2.5
$\bar{g}_{CAN}$ (mS/cm^2)	Frequency (Hz)
0.25	10.0
0.10	10.0
0.05	4.2
0.0	3.1

The decay time of inhibitory postsynaptic currents was varied from $GABA_A$ (β = 0.1 ms^{-1}) to $GABA_B$ (β = 0.003 ms^{-1}) type of synaptic currents, with $\bar{g}_{CAN}$ = 0.25 mS/cm^2 (*above*). The conductance of I_{CAN} was progressively reduced with a $GABA_A$ decay time of β = 0.1 ms^{-1} (*below*). All other parameters were identical to those used in Fig. 2.

recordings. Spatial integration within the dendrites of RE cells could be important for the generation of their bursting behavior (Contreras et al., 1993), but dendrites were not included in the model. Nonetheless, the model exhibited many of the properties observed from intracellular recordings of these cells during spindling.

At the single-cell level, our model of the TC cell shows that two currents, I_T and I_h, can organize various types of slow oscillatory behavior (Destexhe et al., 1993a). In the RE cell, the combination of I_T and $I_{K[Ca]}$ can generate robust oscillation (Wang and Rinzel 1993) and we have observed the same basic behavior with different models of these two currents. In addition, we have found that the magnitude of I_{CAN} controls the frequency of the rhythmic bursting in the range of 8–10 Hz.

At the network level, the simple model presented here allowed us to identify the key elements which may be responsible for 8–10 Hz spindling. (*a*) The slow repetition rate of spindling (0.025–0.1 Hz) is due to mechanisms intrinsic to the TC cell, as shown elsewhere for the waxing and waning slow oscillations (Destexhe et al., 1993a). (*b*) The spindle starts in the TC cell, due to intrinsic oscillatory properties of these neurons. (*c*) The termination of the spindle is due to the Ca^{2+}-induced shift in the voltage dependence of I_h. (*d*) The frequency of spindling (7–14 Hz) is determined by the intrinsic properties of RE cells, as shown by the slower frequency of spindling obtained after blocking I_{CAN} in the RE cell. The frequency of spindling also depends on the kinetics of IPSPs generated by the RE cells, but the maintenance of the oscillation requires the excitatory feedback from TC cells. Therefore, in this model, spindle oscillations are due to the interplay of the intrinsic properties of both types of cells, similar to a suggestion of McCormick (1992).

The model makes several predictions that could be tested from intracellular recordings of TC cells during spindling. First, during the silent period, the membrane should slowly hyperpolarize by a few millivolts. This has already been shown to be a characteristic of waxing and waning slow oscillations in vitro (Leresche et al., 1991). Second, because spindle termination in the model depends on the Ca^{2+} regulation of I_h in TC cells, spindle waves should be sensitive to the alteration of either I_h or intracellular Ca^{2+}. Third, the

frequency of spindle rhythmicity should depend on the kinetics of the decay phase of inhibitory synaptic currents. Finally, the model predicted that the frequency of spindling also depends on the intrinsic properties of the RE cell. Selectively blocking I_{CAN} resulted in a slowing down of the spindle frequency.

Our model of a single pair of interconnected TC and RE cells lacks the variability observed in the thalamus itself, although it could, in principle, be tested with tissue culture experiments similar to those based on excised and cultured invertebrate neurons (Kleinfeld et al., 1990; Nicholls and Hernandez, 1989; Syed et al., 1990). Nonetheless, the model may provide the kernel of the mechanism that underlies spindling in a network or TC and RE cells. The spatial distribution and the probabilistic nature of real spindling await an appropriate network model (Destexhe et al., 1993c). Such a model should also consider the interactions between RE cells, which constitutes another possible generator of spindle rhythmicity (Destexhe et al., 1993b; Steriade et al., 1987; Wang and Rinzel, 1993).

We acknowledge Drs. Diego Contreras and Mircea Steriade for stimulating discussions and Thierry Bal and John Huguenard for use of their data.
This research was supported by the Howard Hughes Medical Institute, the National Institutes of Health, and the Office for Naval Research.

REFERENCES

Avanzini, G., M. de Curtis, F. Panzica, and R. Spreafico. 1989. Intrinsic properties of nucleus reticularis thalami neurons of the rat studied in vitro. *J. Physiol. (Lond.)*. 416:111–122.

Bal, T., and D. A. McCormick. 1993. Mechanisms of oscillatory activity in guinea-pig nucleus reticularis thalami *in vitro*: a mammalian pacemaker. *J. Physiol. (Lond.)*. 468:669–691.

Curró Dossi, R., A. Nunez, and M. Steriade. 1992. Electrophysiology of a slow (0.5–4 Hz) intrinsic oscillation of cat thalamocortical neurons *in vivo*. *J. Physiol. Lond.* 447:215–234.

Contreras, D., R. Curró Dossi, and M. Steriade. 1993. Electrophysiological properties of cat reticular thalamic neurons *in vivo*. *J. Physiol. (Lond.)*. 470:273–294.

Destexhe, A., and A. Babloyantz. 1993. A model of the inward current I_h and its possible role in thalamocortical oscillations. *NeuroReport*. 4: 223–226.

Destexhe, A., A. Babloyantz, and T. J. Sejnowski. 1993a. Ionic mechanisms for intrinsic slow oscillations in thalamic relay neurons. *Biophys. J.*, 65: 1538–1552.

Destexhe, A., D. Contreras, T. J. Sejnowski, and M. Steriade. 1993b. A model of spindle rhythmicity in the isolated thalamic reticular nucleus. *Institute for Neural Computation Technical Report Series* no. INC-9308.

Destexhe, A., W. W. Lytton, T. J. Sejnowski, D. A. McCormick, D. Contreras, and M. Steriade. 1993c. A model of 7–14 Hz spindling in the thalamus and thalamic reticular nucleus: interaction between intrinsic and network properties. *Soc. Neurosci. Abstr.* 19:516. (Abstr.)

Destexhe, A., Z. Mainen, and T. J. Sejnowski. 1994. An efficient method for computing synaptic conductances based on a kinetic model of receptor binding. *Neural Computation*. 6:14–18.

Hines, M. 1993. NEURON—a program for simulation of nerve equations. *In* Neural Systems: Analysis and Modeling. F. Eeckman, editor. Kluwer Academic Publishers, Norwell, MA. 127–136.

Huguenard, J. R., and D. A. Prince. 1992. A novel T-type current underlies prolonged Ca^{2+}-dependent bursts firing in GABAergic neurons of rat thalamic reticular nucleus. *J. Neurosci.* 12:3804–3817.

Jahnsen, H., and R. R. Llinàs. 1984. Ionic basis for the electroresponsiveness and oscillatory properties of guinea-pig thalamic neurons *in vitro*. *J. Physiol.* 349:227–247.

Kleinfeld, D., F. Raccuia-Behling, and H. J. Chiel. 1990. Circuits constructed from identified Aplysia neurons exhibit multiple patterns of persistent activity. *Biophys. J.* 57:697–715.

Leresche, N., S. Lightowler, I. Soltesz, D. Jassik-Gerschenfeld, and V. Crunelli. 1991. Low frequency oscillatory activities intrinsic to rat and cat thalamocortical cells. *J. Physiol. (Lond.)*. 441:155–174.

McCormick, D. A. 1992. Neurotransmitter actions in the thalamus and cerebral cortex and their role in neuromodulation of thalamocortical activity. *Prog. Neurobiol (Oxford)*. 39:337–388.

McCormick, D. A., and H. C. Pape. 1990. Properties of a hyperpolarization-activated cation current and its role in rhythmic oscillations in thalamic relay neurons. *J. Physiol. (Lond.)*. 431:291–318.

Nicholls, J. G., and U. G. Hernandez. 1989. Growth and synapse formation by identified leech neurons in culture: a review. *Q. J. Exp. Physiol.* 74: 965–973.

Otis, T. S., Y. Dekoninck, and I. Mody. 1993. Characterization of synaptically elicited $GABA_B$ responses using patch-clamp recordings in rat hippocampal slices. *J. Physiol. (Lond.)*. 463:391–407.

Soltesz, I., S. Lightowler, N. Leresche, D. Jassik-Gerschenfeld, C. E. Pollard, and V. Crunelli. 1991. Two inward currents and the transformation of low frequency oscillations of rat and cat thalamocortical cells. *J. Physiol. (Lond.)*. 441:175–197.

Steriade, M., and M. Deschênes. 1984. The thalamus as a neuronal oscillator. *Brain Res. Rev.* 8:1–63.

Steriade, M., L. Domich, G. Oakson, and M. Deschênes. 1987. The deafferented reticular thalamic nucleus generates spindle rhythmicity. *J. Neurophysiol. (Bethesda)*. 57:260–273.

Steriade, M., and R. R. Llinàs. 1988. The functional states of the thalamus and the associated neuronal interplay. *Physiol. Rev.* 68:649–742.

Syed, N. I., A. G. Bulloch, and K. Lukowiak. 1990. In vitro reconstruction of the respiratory central pattern generator of the mollusk *Lymnaea*. *Science (Washington DC)*. 250:282–285.

Traub, R. D., and R. Miles. 1991. Neuronal Networks of the Hippocampus. Cambridge University Press, Cambridge.

von Krosigk, M., T. Bal, and D. A. McCormick. 1993. Cellular mechanisms of a synchronized oscillation in the thalamus. *Science (Washington DC)*. 261:361–364.

Wang, X. J., and J. Rinzel. 1993. Spindle rhythmicity in the reticularis thalami nucleus—synchronization among inhibitory neurons. *Neuroscience*. 53:899–904.

Wang, X. J., J. Rinzel, and M. A. Rogawski. 1991. A model of the T-type calcium current and the low-threshold spike in thalamic neurons. *J. Neurophysiol. (Bethesda)*. 66:839–850.

Yamada, W. M., C. Koch, and P. R. Adams. 1989. Multiple channels and calcium dynamics. *In* Methods in Neuronal Modeling. C. Koch and I. Segev, editors. MIT Press, Cambridge, MA. 97–134.